ACS Macro Letters

Letter

pubs.acs.org/macroletters

Molecular Mechanism of Moisture-Induced Transition in Amorphous Cellulose

Karol Kulasinski,*[,†] Sinan Keten,[‡] Sergey V. Churakov,[§] Robert Guyer,[∥,⊥] Jan Carmeliet,[†,#] and Dominique Derome[#]

[†]Swiss Federal Institute of Technology Zürich, Stefano-Franscini-Platz 5, 8093 Zürich, Switzerland

[‡]Department of Civil and Environmental Engineering, Department of Mechanical Engineering, Northwestern University, 2145 Sheridan Road, Evanston, Illinois 60208-3109, United States

[§]Laboratory for Waste Management, Paul Scherrer Institute, 5232 Villigen PSI, Switzerland

[∥]Solid Earth Geophysics Group, Los Alamos National Laboratory, MS D446, Los Alamos, New Mexico 87545, United States

[⊥]Department of Physics, University of Nevada, Reno, Nevada 89557, United States

[#]Laboratory of Building Science and Technology, Empa, Swiss Federal Laboratories for Materials Science and Technology, Überlandstrasse 129, 8600 Dübendorf, Switzerland

ABSTRACT: We investigate the influence of adsorbed water on amorphous cellulose structure and properties, within the full range of moisture content from the dry state to saturation, by molecular dynamics simulation. Increasing water content results in overall swelling, a substantial decrease in stiffness, and higher diffusivity of the water molecules. The obtained sorption curve as well as the range of swelling and weakening are confirmed by experiments. The measured properties undergo a noticeable change at about 10% of moisture content, which suggests that a transition occurs in the porous system, indicating that the sorption process is stepwise. Our analysis of water network formation reveals that the onset of percolation coincides with the moisture content at which a transition in the material properties is observed. An in-depth analysis of the molecular mechanism of hydrogen bonding, van der Waals interactions, and water network in the two regimes enhances the understanding of the adsorption process.

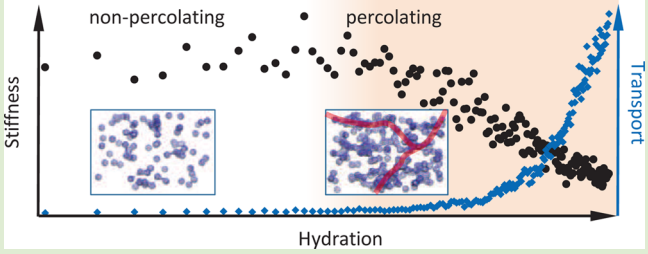

Wood, when exposed to moisture, undergoes changes in its geometric structure as well as in its physical and mechanical properties. The source for this moisture dependence lies in its noncrystalline constituents, such as amorphous cellulose (AC), a hydrophilic polymer found mainly in the outer regions of crystalline cellulose fibers.[1,2] Because of its porous structure and the presence of exposed hydroxyl sites of glucopyranose rings, AC is hydrophilic and a water adsorber. The adsorbed water is known to rearrange the structure of AC and to drive changes in its mechanical properties and geometry.[2,3] While the structure of dry AC is well-known,[4] the process of moisture sorption, being the subject of this paper, has yet to be elucidated. The moisture sorption process occurs at the atomic scale, and consequently molecular dynamics (MD) simulations are an appropriate tool for investigation.[5]

Moisture-induced swelling and weakening, measurable at a macroscopic level,[1,6] lead themselves particularly well to be observed at the atomistic scale. The swelling and weakening have been hitherto considered linear processes.[7] Behavior different from linear, observed experimentally at very low moisture content, is often excused on the grounds of data uncertainty.[8] MD simulations presented in this Letter reveal the existence of two regimes, separated by a transition region, that can be observed in many properties when plotted as a function of moisture content and that have not been reported before. Employing an original *constant-moisture content* simulation technique we answer the question of why sorption in AC is a nonlinear process and what is its atomic origin. Finally, we will show that the percolation of a water network occurs at the transition between the two regimes where the properties we have measured undergo marked changes in behavior.

In our simulation protocol, the amorphous cellulose systems are formed from unconstrained crystalline chains[5] using the same simulation conditions as in ref 5. The system is raised to a high temperature, 700 K, in vacuum, where the chains are allowed to amorphize, and then quenched to 300 K. The calculations are done using a thermostat and barostat following Hamiltonian dynamics in order to ensure the right measurements of dynamical properties. The resulting systems have nominal volume up to 40 nm^3 and comprise 2−4 cellulose chains equivalent to 160−180 glucopyranose units. Throughout

Received: August 26, 2014
Accepted: September 26, 2014
Published: September 30, 2014

   dx.doi.org/10.1021/mz500528m | *ACS Macro Lett.* 2014, 3, 1037−1040

the simulation they are maintained at 300 K and pressure, p = 0. The AC systems are loaded with water molecules, by an insertion method described below, to a moisture content, m, between 0% and 50%, m = (mass of H_2O)/(mass of dry AC). We determine the H_2O equation of state, i.e., m vs chemical potential, μ, and we measure the swelling strain ϵ_s, the bulk modulus K, and the H_2O diffusion constant D, as a function of m. The simulations are carried out using the GROMOS 53a6 united atom force field[9] with periodic boundary conditions and long-range Coulomb interactions.

In order to form the $m > 0$ systems, simple point-charge (SPC) H_2O molecules are placed at random positions with random orientation. If the van der Waals radii of the placed molecule and of the other molecules do not overlap, the insertion is accepted and followed by a 1 ps equilibration. The insertion is repeated until a desired moisture content value is reached and then equilibrated for 1 ns. In this way the system can be loaded to approximately 800 H_2O molecules, corresponding to m = 50%. Measurements of the properties of the system are conducted at values of m that are spaced by Δm = 0.3%. The results reported are the average over three independent systems in order to improve the statistics.

We note that a Monte Carlo simulation would sample the phase space better; however, the high density of the system makes the insertion highly inefficient. We decided therefore to use MD with sufficient simulation time, in order to ensure good sampling, according to the ergodicity theorem.[10]

We begin the study of the H_2O–AC system with the equation of state of the H_2O–AC, the m–μ relationship. The value of μ equals to the free energy of H_2O insertion under constant volume and temperature conditions. Among numerous methods that estimate free energy, the one-step perturbation method is chosen, as it meets the criteria of the simulated system and is not very time-consuming.[11] In order to get free energy estimation, the Zwanzig formula[12] is applied. We show the results in Figure 1 as m vs RH, where RH is the

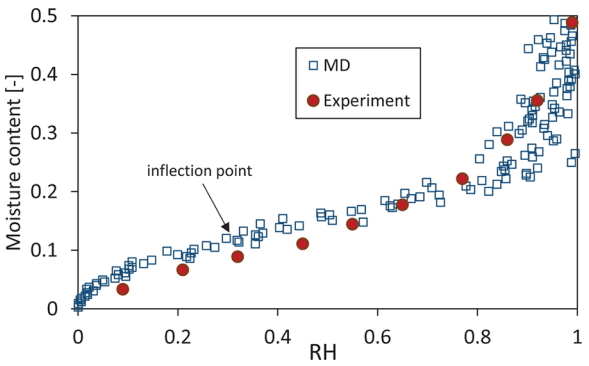

Figure 1. Adsorption curve of amorphous cellulose measured by MD and experimentally. The inflection point of the model curve occurs at m = 11%.

relative humidity, the conventional surrogate for μ, and k_BT ln(RH) = $\mu - \mu_{sat}$ (μ_{sat} is the chemical potential of saturated vapor). On this figure we also show the measurements of Beever and Valentine[13] as closed circles. The good agreement between the simulation results and experiment is gratifying. In Figure 2 we show μ as a function of m. We note a qualitative change in the behavior of μ as a function of m at $m \approx$ 0.1. We will look at this point as we move on.

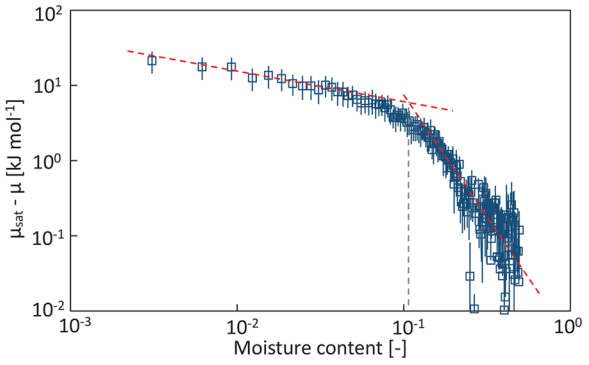

Figure 2. Relative value of the chemical potential, $\mu_{sat} - \mu$, of adsorbed water measured vs moisture content, m. The rate of decrease of the chemical potential changes near m = 11%.

The most apparent macroscopic consequence of having AC in the presence of H_2O is that it takes up water and it swells. To measure the swelling strain, defined by

$$\epsilon_{swelling}(m) = \frac{V(m) - V(0)}{V(0)} \quad (1)$$

where $V(m)$ is the volume of the system at moisture content m, we monitor the volume of AC as it is loaded with moisture. The results are shown in Figure 3a. We note that the swelling curve becomes linear at $m \approx 0.1$.

We next turn to measurement of the undrained bulk modulus of the system as a function of m. We implement the definition

$$K(m) = -V(m)\left(\frac{\partial \sigma}{\partial V}\right)_{T,m} \quad (2)$$

by applying a uniform stress of 100 MPa and measuring the resulting volume change. Up to this stress the system still remains in the linear domain. The results are shown in Figure 3b. Note the abrupt change in the behavior of K vs m at $m \approx$ 0.1.

For a final measurement of the behavior of the system we turn to a transport coefficient. We measure the diffusion constant as a function of m. At each m we study the mean-square displacement of all the H_2O molecules in the system as a function of time in its linear regime. We report the values of diffusion coefficient

$$D = \lim_{n \to \infty} \frac{\langle (x - x_0)^2 \rangle}{6t} \quad (3)$$

as $D(m)$ in Figure 4. As with μ, ϵ_{swell}, and K we see that there is a qualitative change in behavior of D at $m \approx$ 0.1.

It is apparent that there is an important change in the response of the AC to moisture when the moisture content exceeds about 10%. In order to examine what is going on, we undertake a study of the structure of the H_2O network that resides in the AC system as m increases.

We expect the change in response of the AC system to moisture to be related to the configuration of the H_2O system in the AC. As a first look at this system, we examine the water density profiles (Figure 5a–d) for various values of m. These profiles are obtained, with the system in thermal equilibrium, by averaging water molecule positions over 1 ns. At low m the water forms "islands". As m increases separated clusters start to merge. In order to provide an in-depth analysis of the

dx.doi.org/10.1021/mz500528m | ACS Macro Lett. 2014, 3, 1037–1040

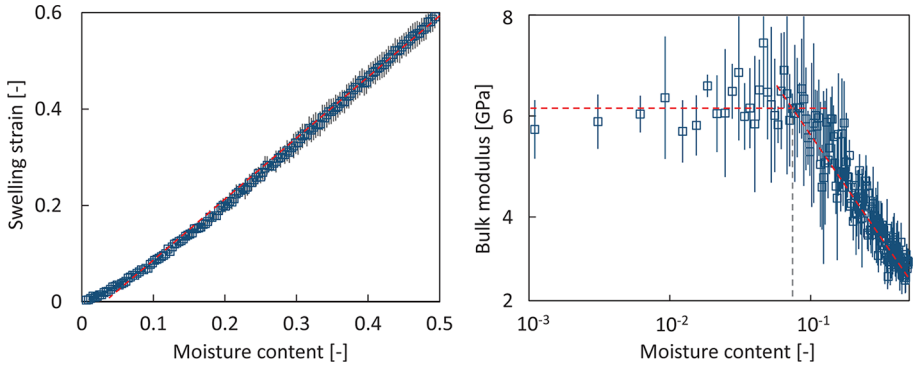

Figure 3. (a) Two stages of volumetric swelling of amorphous cellulose. Swelling vs moisture content is strictly linear above m = 10%. (b) Decrease of bulk modulus. Initially unaffected, the material loses its stiffness after the m = 8% threshold.

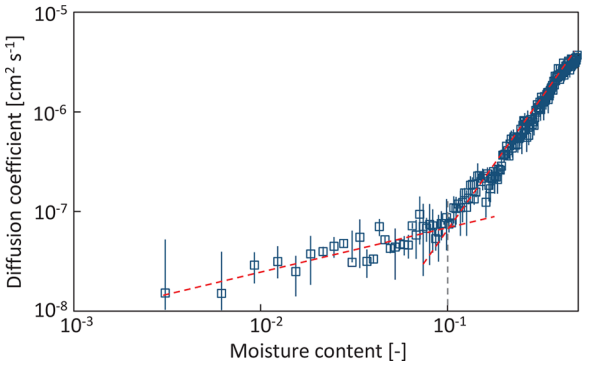

Figure 4. Diffusion coefficient of water molecules vs moisture content reveals the existence of two regimes.

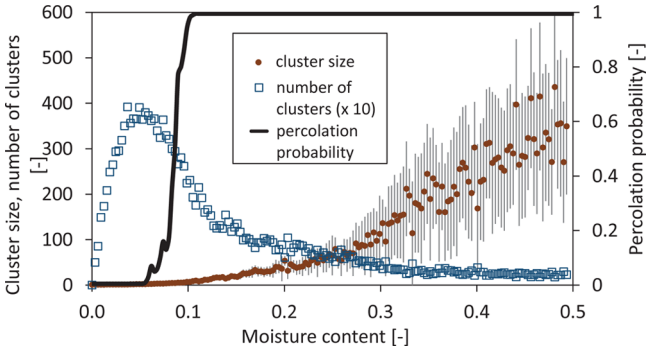

Figure 6. Number of clusters, average cluster size, and percolation probability vs moisture content show two regimes: up to m = 10% the number of clusters increases, cluster size is up to a few molecules, and the H_2O network is not percolating. Above that value, the percolation is more likely to occur and the clusters merge.

configurations of the H_2O we undertake a study of H_2O clusters. The definition of a water molecule cluster is distance-based. For each molecule in a cluster, the distance of its oxygen to the oxygen of the nearest water molecule is less than the parameter d_0. We choose d_0 = 0.6 nm, corresponding to the second minimum of the radial distribution function of SPC water. We show the average size of clusters in the periodic box and the number of clusters as a function of m in Figure 6. Up to m = 0.08 the number of clusters increases, while the average size of a cluster is below 10 H_2O molecules. Once in the second regime, the number of clusters decreases due to merging, and the average size of a cluster increases quickly as plotted vs m. Note the increasing standard deviation of cluster size.

We also show the probability of the percolation of the system of clusters as a function of m in Figure 6. This probability comes from the time average over the 1 ns trajectory. In a given configuration, the value of percolation is binary (exists or not); however, it can also be a fraction, when averaged over many configurations. The network percolates when there is at least one cluster that spans the box which, in terms of periodic

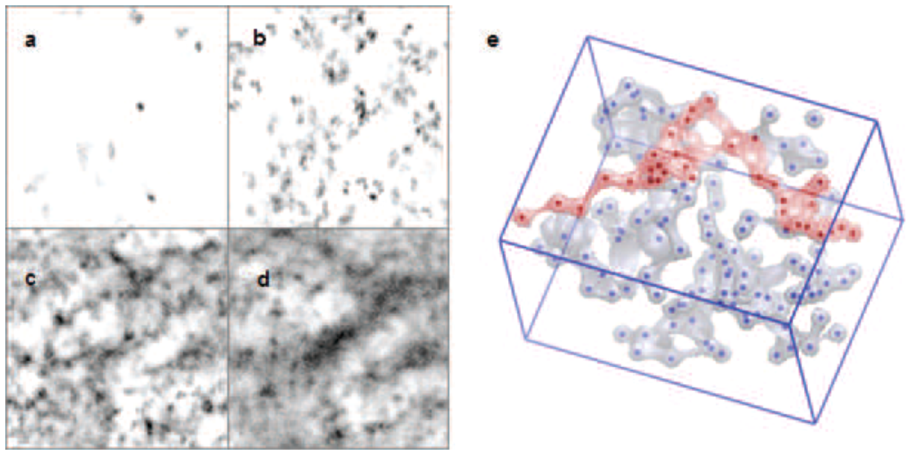

Figure 5. Density profiles of the water phase (dark), showing merging clusters, at 1% (a), 6% (b), 35% (c), and 50% (d) of moisture content. (e) Water network at m = 8%: the percolating cluster is red-highlighted.

dx.doi.org/10.1021/mz500528m | ACS Macro Lett. 2014, 3, 1037−1040

boundary conditions, means that there is at least one infinite network of water molecules. The water is found to percolate at m = 0.09 (where the probability exceeds 50%). It is at this moisture content that the properties we have measured undergo marked changes in behavior. Thus, the configuration of the H_2O system (network) is importantly involved in determining this behavior.

In this Letter we presented a consistent framework to investigate the adsorption in porous materials using atomistic simulations. We have shown that, at low moisture content, a state difficult to obtain in experiments without damaging/changing the material, the behavior of a porous material is different than at higher moisture content. Near the percolation threshold, we saw many properties of the H_2O−AC system undergoing a qualitative change.

The moisture content, at which the H_2O network starts to percolate, separates the two regimes. The low moisture content regime, up to the inflection point of the sorption curve, is characterized by low diffusion, little swelling, and no change in elastic modulus. The water clusters comprise up to 10 water molecules, and the number of clusters increases with moisture content. The H_2O molecules are mainly located in the existing voids, strongly bonded to the cellulose sorption sites. This causes the molecular transport to be very slow, resulting in small diffusion coefficient. The water present in AC does not weaken the van der Waals and Coulomb interactions and causes little swelling; hence, it does not influence the bulk modulus.

Above m = 0.1 the H_2O network percolates and the system enters the second regime. The clusters start to merge, decreasing in number and increasing in size. A linear swelling curve is measured as the adsorbed water molecules push away the cellulose chains, thus making space for more H_2O molecules, and every inserted molecule increases the volume equally. Swelling occurs because the solvation pressure of the fluid is significantly larger than the bulk pressure and results from an interplay between adsorption energy, steric repulsion, and cohesive forces, such as van der Waals or H-bonds.

In contrast to swelling, the decrease in stiffness is a more complex process. It involves breaking of hydrogen bonds and weakening van der Waals and Coulomb interactions, by increasing the chain-to-chain distance, as well as an increase in the surface area of the voids occupied by water. This kind of softening behavior has been already observed experimentally in other systems interacting with moisture.[6,14]

Apart from water trapped at the sorption sites, there are molecules that are not so strongly bonded to cellulose. This, in turn, leads to greater mobility and thus an increase of the diffusion coefficient, such that a H_2O molecule can move through the porous network.[15,16] We note that a slight decrease in diffusion coefficient at high moisture content is measured for some cellulosic materials, such as in refs 17 and 18. However, such data come from measurements on composite materials containing crystalline and noncrystalline cellulose. At high water activities the crystalline cellulose restrains to some degree the increase of porosity which results in a higher effective density of the sorbed water and limits its diffusion. In the case of pure amorphous cellulose, contrary to those containing crystalline cellulose, the swelling is not restrained as the amorphous matrix is soft and can easily yield to increase the volume of the pores. For wood in general, the diffusion coefficient increases with relative humidity throughout the whole range.[16,19−21]

It is remarkable, although maybe fortuitous, that the percolation co-occurs with the observed changes, although there is no direct physical causal effect between the percolation and the change of mechanical properties that are more related to the breaking of hydrogen bonds and other structural changes. The findings present in this paper may motivate further synthesis and design efforts using cellulose as well as synthetic polymers (e.g., hybrid nanocomposites or biomimetic macromolecules).

AUTHOR INFORMATION

Corresponding Author

*E-mail: kulasinski@arch.ethz.ch.

Notes

The authors declare no competing financial interest.

REFERENCES

(1) Derome, D.; Rafsanjani, A.; Patera, A.; Guyer, R.; Carmeliet, J. *Philos. Mag.* **2012**, *92*, 3680−3698.
(2) Engelund, E. T.; Thygesen, L. G.; Svensson, S.; Hill, C. A. *Wood Sci. Technol.* **2013**, *47*, 141−161.
(3) Olsson, A.-M.; Salmen, L.; Eder, M.; Burgert, I. *Wood Sci. Technol.* **2007**, *41*, 59−67.
(4) Mori, T.; Chikayama, E.; Tsuboi, Y.; Ishida, N.; Shisa, N.; Noritake, Y.; Moriya, S.; Kikuchi, J. *Carbohydr. Polym.* **2012**, *90*, 1197−1203.
(5) Kulasinski, K.; Keten, S.; Churakov, S. V.; Derome, D.; Carmeliet, J. *Cellulose* **2014**, *21*, 1103−1116.
(6) Cousins, W. J. *Wood Sci. Technol.* **1978**, *12*, 161−167.
(7) Kollmann, F.; Cote, W. *Principles of wood science and technology*; Springer: New York, 1968.
(8) (US), FPL *Wood handbook: wood as an engineering material*; United States Government Printing: Washington, DC, 1987.
(9) Oostenbrink, C.; Villa, A.; Mark, A. E.; Van Gunsteren, W. F. *J. Comput. Chem.* **2004**, *25*, 1656−1676.
(10) Zhang, X.; Tschopp, M. A.; Horstemeyer, M. F.; Shi, S. Q.; Cao, J. *Int. J. Model., Identif. Control* **2013**, *18*, 211−217.
(11) Pitera, J. W.; van Gunsteren, W. F. *J. Phys. Chem. B* **2001**, *105*, 11264−11274.
(12) Zwanzig, R. W. *J. Chem. Phys.* **1954**, *22*, 1420−1426.
(13) Beever, D. K.; Valentine, L. *J. Polym. Sci.* **1958**, *32*, 521−522.
(14) Sundberg, J.; Toriz, G.; Gatenholm, P. *Polymer* **2013**, *54*, 6555−6560.
(15) Froix, M. F.; Nelson, R. *Macromolecules* **1975**, *8*, 726−730.
(16) Tremblay, C.; Cloutier, A.; Fortin, Y. *Wood Sci. Technol.* **2000**, *34*, 109−124.
(17) Slavutsky, A. M.; Bertuzzi, M. A. *Carbohydr. Polym.* **2014**, *110*, 53−61.
(18) Belbekhouche, S.; Bras, J.; Siqueira, G.; Chappey, C.; Lebrun, L.; Khelifi, B.; Marais, S.; Dufresne, A. *Carbohydr. Polym.* **2011**, *83*, 1740−1748.
(19) Sonderegger, W.; Vecellio, M.; Zwicker, P.; Niemz, P. *Holzforschung* **2011**, *65*, 819−828.
(20) Defo, M.; Fortin, Y.; Cloutier, A. *Wood Fiber Sci.* **1999**, *31*, 343−359.
(21) Araujo, C. D.; Avramidis, S.; MacKay, A. L. *Holzforschung-Int. J. Biol., Chem., Phys. Technol. Wood* **1994**, *48*, 69−74.